The *Culicoides sonorensis* inhibitor of apoptosis 1 protein protects mammalian cells from apoptosis induced by infection with African horse sickness virus and bluetongue virus

Elaine Vermaak[a], Francois F. Maree[a, b] and Jacques Theron[a, *]

[a] Department of Microbiology and Plant Pathology, University of Pretoria, Pretoria, South Africa, 0002

[b] Transboundary Animal Diseases, Onderstepoort Veterinary Institute, Agricultural Research Council, Pretoria, 0110, South Africa

***Corresponding author:** Prof Jacques Theron
Email: jacques.theron@up.ac.za
Telephone: +27 12 420-2994
Fax: +27 12 420-3266

ABSTRACT

African horse sickness virus (AHSV) and bluetongue virus (BTV) are arboviruses of the genus *Orbivirus* that are transmitted to their vertebrate hosts by *Culicoides* biting midges. These orbiviruses exhibit lytic infection (apoptosis) in mammalian cells, but cause persistent infection with no cytopathic effects in *Culicoides sonorensis* cells. Although regulation of apoptosis could thus be integral for establishing persistent virus infection in midge cells, nothing is known about the presence and function of apoptosis pathways in *Culicoides* midges and their derived cell lines. Here, we report the cloning and functional characterization of an inhibitor of apoptosis protein (IAP), designated CsIAP1, from *C. sonorensis* cells. The CsIAP1 protein contains two baculoviral IAP repeat (BIR) domains and a RING domain. Silencing of the Cs*iap*1 gene in *C. sonorensis* cells caused apoptosis, indicating that CsIAP1 plays a role in cell survival. Stable expression of the CsIAP1 protein in BSR mammalian cells suppressed apoptosis induced by AHSV-4 and BTV-10 infection, and biochemical data indicated that CsIAP1 is an inhibitor of mammalian caspase-9, an initiator caspase in the intrinsic apoptotic pathway. Mutagenesis studies indicated that the BIR2 and RING domains are required for the anti-apoptotic activity of CsIAP1. The results suggest that the mechanism by which CsIAP1 suppresses apoptosis in insect cells may involve inhibition of a *Culicoides* caspase-9 homologue through a mechanism that requires both the BIR2 and RING domains. This study provides the first evidence that the CsIAP1 protein is a key negative regulator of apoptosis in *C. sonorensis* cells.

Keywords:
orbivirus; *Culicoides sonorensis*; apoptosis; inhibitor of apoptosis; African horse sickness virus; bluetongue virus

1. Introduction

African horse sickness virus (AHSV) and bluetongue virus (BTV) are arboviruses belonging to the genus *Orbivirus* (family *Reoviridae*). AHSV causes severe disease in horses with a mortality rate of up to 95% (Stassen et al., 2014), while BTV is one of the most economically important arboviruses of domesticated ruminants (Wilson and Mellor, 2009). The respective viral genomes are composed of 10 segments of linear double-stranded RNA (dsRNA), which encode four nonstructural proteins (NS1 to NS4) and seven structural proteins. The structural

proteins VP1, VP3, VP4, VP6 and VP7 form the icosahedral virus core-particle, which is surrounded by an outer capsid layer composed of VP2 and VP5 (Roy, 2008; Manole et al., 2012).

Both AHSV and BTV are transmitted between their respective vertebrate hosts by biting haemotophageous midges of the *Culicoides* genus. Although AHSV and BTV are able to replicate in both the vector insect and their vertebrate hosts, severe disease is only caused in the host animals (Mellor and Mertens, 2009; Wilson et al., 2009). This is also reflected in tissue culture where infection of midge-derived cell cultures is unapparent and shows little or no cytopathic effect (CPE). In contrast, virus-infected mammalian cell cultures show strong CPE that correlates with the amount of apoptosis in the cells (Mortola et al., 2004; Stassen et al., 2012). Although apoptotic pathways induced in mammalian cells by orbivirus infections have been characterized (Stewart and Roy, 2010; Vermaak and Theron, 2015), there is a paucity of information regarding apoptosis and apoptosis regulation in *Culicoides* midges and their derived cell lines.

Apoptosis is a genetically controlled mechanism of cell death that is important in development, tissue homeostasis and innate immunity. Apoptotic cells are characterized by nuclear chromosomal condensation and fragmentation, cell membrane blebbing and formation of apoptotic bodies (Wyllie, 1997; Timmer and Salvesen, 2007). These features of apoptosis are caused by caspases, a family of cysteine proteases that are activated following an apoptotic response (Li and Yuan, 2008; Chowdhury et al., 2008). A core apoptotic pathway exists in nematodes, insects and vertebrates (referred to as the intrinsic pathway in vertebrates), which regulates apoptosis by controlling the activation of caspases. In broad terms, the core apoptotic pathway controls the activation of initiator caspases, which occurs by formation of the apoptosome, a complex that promotes initiator caspase dimerization. Activated initiator caspases cleave and activate effector caspases, which cleave numerous cellular substrates, leading to the stereotypical morphological changes associated with apoptosis (Hay and Guo, 2006; Elmore, 2007; Liu and Clem, 2011). The major components of the core apoptotic pathway are largely conserved among metazoans, but there are some differences in how caspase activation is regulated (Tenev et al., 2005).

In many animal species, including nematodes, insects, mammals and humans, the main negative regulators of caspases are inhibitor of apoptosis (IAP) proteins (Salvesen and

Duckett, 2002; Berthelet and Dubrez, 2013). All IAP proteins have a distinctive primary structure. They are characterized by the presence of one to three baculovirus IAP repeat (BIR) domains in the amino (N)-terminal region and most also contain a RING (Really Interesting New Gene) finger domain in the carboxyl (C)-terminal region (Mace et al., 2010). The BIRs, which consist of approximately 70-80 amino acids, mediate protein-protein interactions and interact with diverse proteins, including caspases. Studies have shown that several human IAP proteins such as XIAP, c-IAP1 and c-IAP2, can directly bind and inhibit caspase-3, caspase-7 and caspase-9 (Roy et al., 1997; Deveraux et al., 1997). The IAP proteins of *D. melanogaster* (DIAP1), *Aedes aegypti* (AeIAP1) and *Ae. albopictus* (AaIAP1) also inhibit some caspases (Muro et al., 2002; Li et al., 2007; Liu and Clem, 2011). The RING domain of IAP proteins consists of approximately 40 amino acids and functions as an E3 ubiquitin ligase, which promotes transfer of ubiquitin to selected protein targets, including caspases. Thus, the IAP proteins are also implicated in the proteasome-mediated degradation of target proteins (Wilson et al., 2002; Vaux and Silke, 2005; Ditzel et al., 2008).

Although IAP proteins of *Drosophila* and *Aedes* have been characterized, no apoptosis regulating genes of *Culicoides* had been identified prior to this and another recent related study (Mills et al., 2015). Introduction of *Culicoides sonorensis* IAP dsRNA into adult midges resulted in the death of the midges, but a role in apoptosis has not been directly established (Mills et al., 2015). Here, we report the functional characterization of an *iap* gene from a cell line derived from *C. sonorensis*. The results indicate that the encoded CsIAP1 protein inhibits apoptosis in *C. sonorensis* cells, and suppressed apoptosis induced by AHSV and BTV infection of cultured mammalian cells. Moreover, functional analyses of the CsIAP1 protein indicated that it is an inhibitor of mammalian caspase-9 by a mechanism that requires both the BIR2 and the RING domains.

2. Materials and methods

2.1. Cells and viruses

BSR, a clone of BHK-21 cells (Pretorius et al., 2015), were maintained at 37°C and 5% CO_2 in Eagle's Minimum Essential Medium (EMEM) supplemented with Earle's Balanced Salt Solution (EBSS), 2 mM L-glutamine, 1% (v/v) non-essential amino acids (NEAA), 5% (v/v) foetal bovine serum (FBS), and antibiotics (penicillin, streptomycin and amphotericin B)

(HyClone). Stable BSR cell lines expressing full-length or mutant CsIAP1 were maintained in the same manner as BSR cells with the addition of 500 µg/ml of Geneticin (Invitrogen). The KC cells used were originally derived from *Culicoides sonorensis* (*variipennis*) embryos (Wechsler et al., 1989) and were grown at 28°C in Schneider's Drosophila medium supplemented with 10% (v/v) FBS and antibiotics (Lonza).

AHSV serotype 4 (AHSV-4) and BTV serotype 10 (BTV-10) were used for cell infections. Cell monolayers were rinsed twice with incomplete EMEM (lacking FBS and antibiotics) and then infected with AHSV-4 or BTV-10 at a multiplicity of infection (MOI) of 1 pfu/cell. Virus adsorptions were performed at 37°C for 1 h, followed by incubation in complete EMEM.

2.2. 3' RACE (rapid amplification of cDNA ends)

Total RNA was extracted from KC cells with the Nucleospin RNA II kit (Macherey-Nagel) according to the manufacturer's instructions. An aliquot of total RNA (1 µg) was mixed with 20 µM of poly(A) tail-specific primer (5'-GGCCACGCGTCGACTAGTACTTTTTTTTTTTTTTT-3') and heated at 70°C for 10 min. After chilling on ice, the RNA was reverse transcribed at 42°C for 1 h using the RevertAid H Minus First Strand cDNA synthesis kit (Thermo Scientific). PCR amplifications were subsequently performed using 1 µl of cDNA template and 10 µM of one of three different forward degenerate primers (5'-GTWAAATGYTWYTTCTGYSGMGTGG-3'; 5'-GATCGYGTCMRMTGCTTCAGYTG-3'; 5'-GCTTCAGYTGYGGYGGYGGYCTC-3') designed from conserved regions in published *iap*1 sequences of *D. melanogaster*, *Ae. aegypti*, *Ae. triseriatus* and *Ae. albopictus*, and a reverse primer of which the sequence is complementary to the 5' half of the poly(A) tail-specific primer used in the reverse transcription reaction. The nucleotide sequences of the amplicons were determined using the ABI-PRISM BigDye Terminator Cycle Sequencing Ready Reaction kit v.3.1 (Perkin-Elmer Applied Biosystems), followed by resolution on an ABI-PRISM 3130XL DNA sequencer. Nucleotide sequences were analyzed with the BioEdit v.7.0.4.1 software package (Hall, 1999) and multiple sequence alignments were performed with ClustalW included in the software package.

2.3. 5' RACE

The nucleotide sequence of the 5' end of the Cs*iap*1 mRNA was determined by a series of 5' RACE reactions. In brief, total RNA was extracted from KC cells and reverse transcribed using one of two Cs*iap*1-specific reverse primers (5'-GGAAAAGTAGACTCTCATGACTTTCG-3'; 5'-CATTTTGTGACACTTGACGCAC-3'). cDNAs were purified with the QIAquick PCR Purification kit (Qiagen) and oligo(dC) tails were added to the 3' ends using 30 U of terminal deoxynucleotidyl transferase (Thermo Scientific) in 1 × tailing buffer (1 M potassium cacodylate, 125 mM Tris, 0.05% [v/v] Triton-X-100, 5 mM $CoCl_2$ and 0.025 mM dCTP). Tailing reactions were performed at 37°C for 15 min and then terminated by heat-inactivation at 70°C for 10 min. Tailed cDNAs were purified and PCR amplified with a consensus forward primer specific to the C-tailed termini (5'-GACATCGAAAGGGGGGGGGG-3') and one of two reverse primers specific to the Cs*iap*1 cDNA sequence (5'-CATTTTGTGACACTTGACGCAC-3'; 5'-GCTGTACCACATGGCATGTTG-3'). The amplicons obtained were subjected to nucleotide sequencing, as described above.

2.4. Plasmids

The coding region of the Cs*iap*1 gene was PCR amplified from poly(A)-tailed cDNA using a forward primer (5'-CAAGGTACCATGGCTCCTTGTTACAAAGTACT-3'; *Kpn*I restriction enzyme site underlined) and a reverse primer (5'-CCAGAATTCTCAGGAAAAGTAGACTCTCATGAC-3'; *Eco*RI restriction enzyme site underlined). The purified amplicon was digested with both *Kpn*I and *Eco*RI, and then cloned into the corresponding sites of the pcDNA3.1(+) mammalian expression vector (Invitrogen) to generate pcDNA-Cs*iap*1. The insertion was confirmed by both restriction enzyme digestion and nucleotide sequencing.

Plasmids encoding CsIAP1 proteins lacking the BIR1 (residues 73-143), BIR2 (residues 228-300) or RING (residues 367-401) domain were generated by inverse PCR using the pcDNA-Cs*iap*1 recombinant plasmid as a template and 5'-CGTGAAACTAGTAATGAGCCAATTGATG-3' (BIR1), 5'-ATGAAAGGTCAAGAGTTTATTGATGAAATATTG-3' (BIR2), 5'-AGACAACCATTCACGAAAGTCATGAG-3' (RING) as the forward primer, and 5'-

GAGGCCCGTTATTGTTG-3' (BIR1), 5'-TTCCGGATGTTCATTCCGG-3' (BIR2), 5'-CATTTTGCTGTCACTAACTGCGGC-3' (RING) as the reverse primer. The derived recombinant plasmids were designated as pcDNA-ΔBIR1, pcDNA-ΔBIR2 and pcDNA-ΔRING, respectively. The constructs were verified by nucleotide sequencing.

2.5. Development of stable BSR cell lines for expression of full-length and mutant Csiap1 genes

BSR cells were grown to 80% confluency in 6-well tissue culture plates and transfected with the different recombinant pcDNA3.1(+) constructs using Lipofectamine LTX reagent (Invitrogen) according to the manufacturer's instructions. At 24 h post-transfection, the cells were washed and incubated for a further 24 h in complete EMEM. The cells were then harvested and replated into a 25-cm^2 tissue culture flask containing 5 ml of selective EMEM (complete growth medium with 500 μg/ml of Geneticin). Individual cell clones were selected and grown into the desired stable cell lines.

2.6. Immunoblot analysis

To confirm expression of the full-length and mutant CsIAP1 proteins, monolayers of the stable BSR cell lines developed above were subjected to immunoblot analysis using an anti-CsIAP1 antibody. The polyclonal antibody was generated by immunizing rabbits with a peptide corresponding to amino acids 22-35 (TFQKHNDEIDNKDNC) of the CsIAP1 protein. Peptide synthesis and antibody production were carried out by GenScript Corp. Proteins in cell lysates were separated by 10% SDS-PAGE and transferred to a Hybond-C nitrocellulose membrane (Amersham Pharmacia Biotech AB) with a semi-dry electroblotter (Hoefer) using standard protocols (Sambrook and Russell, 2001). Protein-A conjugated to horseradish peroxidase (Sigma-Aldrich) was used as the secondary antibody and immunoreactive proteins were detected by an enzyme substrate solution (4-chloro-1-naphtol; BioRad).

2.7. Production of dsRNA

Template for the synthesis of dsRNA corresponding to the CsIAP1 coding region was prepared by PCR using pcDNA-Cs*iap*1 as template together with upstream (5'-

GGATCCTAATACGACTCACTATAGGGATGGCTCCTTGTTACAA-3') and downstream (5'-GGATCCTAATACGACTCACTATAGGGTCAGGAAAAGTAGACTC-3') primers, each bearing a T7 RNA polymerase binding site (underlined). For control dsRNA, the coding region of the AHSV-4 S8 gene was PCR amplified from plasmid pJET-S8 using 5'-GGATCCTAATACGACTCACTATAGGGATGGCAGAGGTCAGAAAG-3' as the forward primer and 5'-GGATCCTAATACGACTCACTATAGGGTCAACCGCTCCCCCCTG-3' as the reverse primer (T7 RNA polymerase binding site underlined). The amplicons were purified from an agarose gel using the Zymoclean Gel DNA Recovery kit (Zymo Research Corp.) and then transcribed to synthesize complementary RNA strands using the AmpliScribe T7 High Yield Transcription Kit (Epicentre Biotechnologies) according to the manufacturer's instructions. Following treatment with RNase-free DNase I (37°C, 15 min), the purified complementary RNA strands were heated to 65°C for 15 min and allowed to cool slowly to room temperature to obtain dsRNA. The dsRNA was stored at -70°C until use.

2.8. RNA interference (RNAi)

KC cells were seeded in 24-well tissue culture plates and incubated overnight at 28°C to reach 80-90% confluency. The following day, the medium was replaced with 500 µl serum-free Schneider's Drosophila medium and 60 µg dsRNA (corresponding to 5×10^{13} dsRNA molecules per gene) was added into the medium. Following incubation at 28°C for 2 h, 500 µl Schneider's Drosophila medium supplemented with 20% (v/v) FBS was added to the cells, thereby bringing the final concentration of FBS to 10% (v/v). Control cells were subjected to the same procedure except that no dsRNA or control (AHSV-4 S8) dsRNA was added. The cells were incubated for different periods of times, as indicated in the figures.

2.9. Semi-quantitative RT-PCR

Total RNA was extracted from mock-treated or dsRNA-treated KC cells with the Nucleospin RNA II kit (Macherey-Nagel) and a 1-µg aliquot of total RNA was used in the first strand cDNA synthesis by making use of the RevertAid H Minus First Strand cDNA synthesis kit. Estimation of relative Cs*iap*1 mRNA levels was performed by PCR in the linear range of amplification using Cs*iap*1 gene-specific primers (5'-ATGGCTCCTTGTTACAAAGTACT-3' and 5'-TCAGGAAAAGTAGACTCTCATGAC-3' as the forward and reverse primer, respectively). The number of PCR cycles was kept in the linear range by testing an increasing

number of amplification cycles (15, 20, 25 and 30 cycles). The PCR conditions subsequently used were: 95°C for 2 min, 25 cycles of 95°C for 30 s, 55°C for 30 s and 72°C for 3 min, followed by a final extension at 72°C for 5 min. RT-PCR was also performed for the Hsp60 housekeeping gene as endogenous reference. The sequences of the Hsp60 (GenBank accession no. U87959.1) gene-specific primers were 5'-AGGACGGTGTAACTGTTGCC-3' (forward) and 5'-AACGCGTTTCATTGCGTCAG-3' (reverse).

2.10. Observation of cell morphological changes

Cells were seeded onto coverslips in 6-well tissue culture plates (1×10^6 cells/well) and either treated with Cs*iap*1 or control dsRNA, or infected with AHSV-4 or BTV-10 at a MOI of 1 pfu/cell. The coverslips were removed at different times after dsRNA treatment or infection, and placed on glass slides in the absence of fixatives and sealants. The samples were examined with a Zeiss Axiovert 200 inverted microscope at a magnification of 20× or 40× and the images were captured with a Nikon DXM 120 digital camera.

2.11. DNA fragmentation analyses

Genomic DNA from KC cells treated with dsRNA was extracted with the Apoptotic DNA-Ladder kit (Roche Applied Science) according to the manufacturer's instructions, and separated by electrophoresis in 1% (w/v) agarose gels containing ethidium bromide. In the case of virus-infected BSR cells, the relative amounts of mono- and oligonucleosomes generated from apoptotic cells were quantified *in vitro* using the Cell Death Detection ELISA^{PLUS} kit (Roche Applied Science) according to the manufacturer's instructions.

2.12. Caspase activity assays

The activity of caspase-3, -8 and -9 was determined with the appropriate ApoTarget Caspase Colorimetric Protease Assay kit (BioSource International) according to the manufacturer's protocol. Untreated and dsRNA-treated cells, as well as uninfected and virus-infected cells were harvested, lysed and clarified by centrifugation. The protein concentration of each cytoplasmic extract was determined with the Quick Start Bradford Protein Assay kit (BioRad) and bovine serum albumin (BSA) as the standard. Each sample (100 µg protein/sample) was mixed with reaction buffer and 4 mM of the appropriate substrate

(DEVD-*p*NA for caspase-3, IETD-*p*NA for caspase-8 and LEHD-*p*NA for caspase-9), and incubated at 37°C for 2 h. The liberated *p*NA was quantified by measuring the absorbance at 405 nm with a Multiskan Go microplate spectrophotometer (Thermo Scientific) and increases in caspase activities calculated.

2.13. Virus growth curves

Confluent BSR and BSR-Cs*iap*1 cell monolayers in 6-well tissue culture plates (1×10^6 cells/well) were infected with AHSV-4 or BTV-10 at a MOI of 0.1 pfu/cell. After virus adsorption, the inocula were discarded, cells were washed with EMEM, and 1 ml of the growth medium was added. At different time points post-infection, the virus titres were determined by plaque assays in BSR cells as described previously (Vermaak et al., 2016).

2.14. Statistical analysis

Data are expressed as means ± standard deviations (SD). Significant differences in mean values were assessed by a two-tailed Student's *t* test. A *P* value of ≤ 0.05 was considered significant.

2.15. Nucleotide sequence accession number

The Cs*iap*1 gene sequence has been submitted to GenBank under the accession number KT246121.

3. Results

3.1. Cloning and characterization of the C. sonorensis Csiap1 gene

The full-length Cs*iap*1 cDNA contains a continuous open reading frame encoding a protein of 414 amino acids and has a predicted molecular mass of 46.58 kDa. Similar to other IAP family members, the CsIAP1 protein contains two BIR domains (BIR1 and BIR2) and a RING domain near its C terminus (Supplementary Fig. S1). The CsIAP1 BIR1 and BIR2 domains, which are separated by 84 amino acids, consist of 71 and 73 amino acids,

respectively, and each contains the signature sequence $CX_2CX_{16}HX_{6-8}C$. The CsIAP1 RING domain consists of 35 amino acids, including a signature sequence comprising seven cysteine residues and one histidine residue (C_3HC_4), and is separated from the BIR2 domain by 66 amino acids. The predicted CsIAP1 amino acid sequence is 44%, 47%, 48% and 47% identical to DIAP1 of *D. melanogaster*, AtIAP1 of *Ae. triseriatus*, AaIAP1 of *Ae. albopictus* and AeIAP1 of *Ae. aegypti*, respectively. The highest regions of amino acid identity localized to the BIR1 (57%), BIR2 (81%) and RING domain (83%).

3.2. Silencing of CsIAP1 in Culicoides sonorensis (KC) cells induces spontaneous apoptosis

In cells from *D. melanogaster*, *Ae. aegypti* and the lepidopteran insect *Spodoptera frugiperda*, RNA interference (RNAi) of the IAP1 orthologues DIAP1, AeIAP1 or Sf-IAP induces spontaneous apoptosis, indicating that continuous expression of the IAP1 protein is necessary to maintain cell viability (Muro et al., 2002; Liu and Clem, 2011). We therefore first examined the effect of RNAi-mediated knockdown of Cs*iap*1 in KC cells. Addition of Cs*iap*1 dsRNA to KC cells resulted in a dramatic reduction in the level of Cs*iap*1 transcripts after 12 h post-treatment and transcripts were not detectable by RT-PCR at 48 h post-treatment. In contrast, treatment with the control (AHSV-4 S8) dsRNA did not have an apparent effect on the Cs*iap*1 transcript levels (Fig. 1A), suggesting that the silencing response was specific. Light microscopy of KC cells treated with Cs*iap*1 dsRNA indicated that by 24 h post-treatment the cells displayed morphological changes associated with apoptosis, such as cell rounding and detachment and the formation of apoptotic bodies, and by 48 h nearly all of the cells had undergone apoptosis. In contrast, cells treated with control dsRNA remained unchanged (Fig. 1B). In addition to the stereotypical morphological changes that accompany apoptosis, the Cs*iap*1 dsRNA-treated cells underwent DNA fragmentation into oligonucleosomal ladders (Fig. 1C), and Cs*iap*1 dsRNA-treated cells contained high levels of effector caspase-3-like activity as measured by cleavage of the effector caspase-3 substrate DEVD-*p*NA (Fig. 1D). These results indicate that silencing of Cs*iap*1 induced apoptosis in KC cells, similar to what has been previously observed in *D. melanogaster* S2 cells, *Ae. aegypti* Aag2 cells and *S. frugiperda* Sf21 cells.

3.3. The CsIAP1 protein is active in rescuing apoptosis induced by AHSV-4 and BTV-10 in mammalian cells

Infection of mammalian cells with AHSV or BTV induces all the classical morphological and biochemical changes indicative of apoptosis at 24 to 48 h post-infection (Mortola et al., 2004; Nagaleekar et al., 2007; Stassen et al., 2012). Since CsIAP1 appears to be necessary to maintain *C. sonorensis* cell viability, we next tested the CsIAP1 protein for its ability to prevent apoptosis in mammalian cells due to virus infection as stimulus. To investigate, BSR cells and BSR-Cs*iap*1 cells, which stably express the full-length CsIAP1 protein (Supplementary Fig. S2), were infected with AHSV-4 or BTV-10 at a MOI of 1 pfu/cell, and analyzed for morphological and biochemical markers of apoptosis at 24 and 48 h after infection.

The results, presented in Fig. 2, indicated that apoptosis was induced in virus-infected BSR cells. With the progression of infection, there was a concomitant increase in cells displaying morphological changes characteristic of apoptosis (cell rounding, shrinkage and detachment), as well as an increase of free nucleosomes released into the cytoplasm of virus-infected cells and an increase in the activity of caspase-3, a key agent of apoptosis in mammalian cells. However, these apoptotic responses were markedly attenuated in virus-infected BSR-Cs*iap*1 cells compared to virus-infected BSR cells. Infection of the BSR-Cs*iap*1 cells with the respective viruses resulted in fewer cells displaying morphological changes that accompany apoptosis as compared to virus-infected BSR cells (Fig. 2A). In contrast to virus-infected BSR cells, the release of free nucleosomes into the cytoplasm of BSR-Cs*iap*1 cells infected with either AHSV-4 or BTV-10 were significantly reduced (Fig. 2B). Moreover, BSR cells infected with AHSV-4 or BTV-10 exhibited high levels of caspase-3 activity, whereas caspase 3 activity was significantly reduced at 48 h post-infection in BSR cells expressing CsIAP (Fig. 2C). Taken together, the data confirm a role for CsIAP1 in promoting cell survival and also indicate that apoptosis induced by AHSV-4 and BTV-10 infection of mammalian cells is suppressed by the anti-apoptotic *C. sonorensis* protein CsIAP1.

3.4. Replication of AHSV-4 and BTV-10 in BSR and BSR-Csiap1 cells

To evaluate the effect of Cs*iap*1 gene expression in BSR-Cs*iap*1 cells on AHSV-4 and BTV-10 replication, the growth curves of each virus were compared in BSR and BSR-Cs*iap*1 cells.

The growth kinetics of the viruses in the BSR and BSR-Cs*iap*1 cells were similar; however, the virus progeny yield was lower in BSR-Cs*iap*1 cells (Fig. 3). At 72 h post-infection, the titre of AHSV-4 in BSR cells was 7.1×10^7 pfu/ml, whereas the titre in BSR-Cs*iap*1 cells was 8.8×10^6 pfu/ml, representing an 8.1-fold reduction in virus titre. For BTV-10, the titre at 72 h post-infection in BSR-Cs*iap*1 cells was 10-fold lower than that in BSR cells (1.3×10^6 and 1.3×10^7 pfu/ml, respectively). These results indicate that while expression of the Cs*iap*1 gene did not completely prevent virus-induced apoptosis in cell culture, virus progeny yields were decreased when a functional Cs*iap*1 gene was expressed.

3.5. CsIAP1 suppresses the intrinsic but not the extrinsic apoptotic pathway in mammalian cells

The results of this study indicated that CsIAP1 is able to suppress apoptosis of mammalian cells induced by AHSV-4 or BTV-10 and coincides with a reduction in caspase-3 activity. In mammals, there are two distinct pathways of caspase activation, the extrinsic and intrinsic pathway. Although these pathways utilize caspase-8 and caspase-9, respectively, as their apical proteases, activated caspase-8 and caspase-9 can each activate the downstream effector caspase, caspase-3 (Elmore, 2007). Thus, to investigate the step at which CsIAP1 acts, we determined the activity of caspase-8 and caspase-9 in BSR and BSR-Cs*iap*1 cells infected with AHSV-4 or BTV-10 at 24 and 48 h after infection.

The activity of caspase-8 was similar in virus-infected BSR and BSR-Cs*iap*1 cells (Fig. 4A), indicating that expression of CsIAP1 had no effect on caspase-8 activity. In contrast, caspase-9 activity was significantly reduced in virus-infected BSR-Cs*iap*1 cells compared to virus-infected BSR cells. At 48 h post-infection, caspase-9 activity was 2.8-fold lower in BSR-Cs*iap*1 cells infected with AHSV-4 than in infected BSR cells. Likewise, caspase-9 activity was reduced 4.5-fold in BSR-Cs*iap*1 cells infected with BTV-10 (Fig. 4B). The results therefore suggest that CsIAP1 suppresses the intrinsic apoptotic pathway in mammalian cells at a step upstream of caspase-3, but does not suppress the extrinsic apoptotic pathway initiated by caspase-8.

3.6. The BIR2 and RING domains of CsIAP1 are required to suppress virus-induced apoptosis in mammalian cells

The CsIAP1 protein possesses two BIRs and a C-terminal RING domain (Supplementary Fig. S1). To investigate the individual contribution of these domains to the anti-apoptotic activity of CsIAP, we generated BSR cell lines that stably express CsIAP1 mutant proteins lacking the BIR1, BIR2 or RING domain (Supplementary Fig. S2). These cell lines were designated as BSR-Cs*iap*1ΔBIR1, BSR-Cs*iap*1ΔBIR2 and BSR-Cs*iap*1ΔRING, respectively. The respective cell lines were subsequently infected with AHSV-4 as apoptotic stimulus and the mutant proteins were evaluated at 48 h post-infection for their ability to suppress virus-induced apoptosis, as well as the activity of caspase-3 and caspase-9.

Light microscopy of the virus-infected cell lines indicated that cell lines expressing the ΔBIR2 or ΔRING domain mutant proteins failed to protect the cells from virus-induced apoptosis. Indeed, these cells displayed morphological changes associated with apoptosis that were comparable to that of control BSR cells infected with AHSV-4 (Fig. 5A). In contrast, markedly fewer cells with characteristics of apoptosis were observed in virus-infected BSR-Cs*iap*1ΔBIR1 cells, and the ΔBIR1 mutant protein was able to suppress virus-induced apoptosis to a seemingly comparable extent than that displayed by the full-length CsIAP1 protein (Fig. 5A). To substantiate the data, the CsIAP1 mutant proteins were next tested for their ability to suppress the activity of effector caspase-3. In agreement with the above results, caspase-3 activity was highest in virus-infected BSR-Cs*iap*1ΔBIR2 and BSR-Cs*iap*1ΔRING cells and the lowest in virus-infected BSR-Cs*iap*1ΔBIR1 cells, which was comparable to the caspase-3 activity in virus-infected BSR-Cs*iap*1 cells (Fig. 5B). Since the results of this study suggested that CsIAP1 suppresses the intrinsic apoptotic pathway at a step upstream of caspase-3, the activity of caspase-9 in the virus-infected cell lines was also evaluated. The results indicated that caspase-9 activity was 2-fold higher in virus-infected BSR-Cs*iap*1ΔBIR2 and BSR-Cs*iap*1ΔRING cells as compared to virus-infected BSR-Cs*iap*1 cells. No statistically significant difference in caspase-9 activity was observed in virus-infected BSR-Cs*iap*1 and BSR-Cs*iap*1ΔBIR1 cells (Fig. 5C). Taken together, these results indicate that both the BIR2 and RING domain regions are required for the anti-apoptotic function of CsIAP1.

4. Discussion

Apoptosis has been shown to be an antiviral response against arboviruses in mosquitoes and is considered to be an important process regulating arbovirus-mosquito interactions (Sim et al., 2014; Clem, 2016). Despite its importance as a vector of several viruses of agricultural importance such as AHSV and BTV, nothing is known about the presence and function of apoptotic pathways in *Culicoides* biting midges or their derived cell lines. To initiate a study of apoptosis, we have cloned, sequenced and functionally characterized an inhibitor of apoptosis gene from *C. sonorensis* cells, designated CsIAP1.

Sequence analysis of the Cs*iap*1 gene indicated that it is a typical IAP, containing two BIR domains and a RING domain. IAP proteins regulate apoptosis by inhibiting initiator and effector caspases, which are essential for cell death, and are therefore considered to be the last line of defence against death-inducing caspase activity (Mace et al., 2010). Consistent with this view, our results indicated that CsIAP1 is a critical regulator of cell survival since silencing of CsIAP1 by RNAi induced apoptosis in cultured *C. sonorensis* cells, as determined by cell morphology, caspase activity and DNA fragmentation. Recently, RNAi-mediated knockdown of CsIAP1 in adult female *C. sonorensis* midges was shown to be associated with accelerated mortality rates (Mills et al., 2015). Taken together, these observations suggest that CsIAP1 may represent a potentially useful target for genetics-based *Culicoides* control strategies (Zhang et al., 2013; Kean et al., 2015) to complement current vector-based control methods such as breeding site removal and the use of traps, repellents and insecticides (Carpenter et al., 2008; Stassen et al., 2014).

To more fully characterize the cell death inhibitory function of CsIAP1, the ability of CsIAP1 to suppress mammalian cell death induced by infection with two different orbiviruses was investigated. Expression of CsIAP1 in BSR mammalian cells attenuated apoptosis caused by AHSV-4 or BTV-10 infection and reduced virus yields (Figs. 2 and 3). These findings suggest that the Cs*iap*1 gene was functional in mammalian cells, albeit that expression of the Cs*iap*1 gene alone was not sufficient to totally block virus-induced apoptosis. Notably, biochemical data indicated that CsIAP1 is an inhibitor of caspase-9, the initiator caspase of the intrinsic apoptotic pathway. Thus, the inability of CsIAP1 expression to completely block virus-induced apoptosis may be ascribed to the ability of BTV and AHSV to induce both the intrinsic and extrinsic apoptotic pathways that exist within mammalian cells (Stewart and

Roy, 2010; Vermaak and Theron, 2015). In the experimental system used in this study, apoptosis could therefore still be induced via the extrinsic pathway despite suppression of the intrinsic apoptosis pathway by CsIAP1. Regardless, the ability of CsIAP1 to suppress apoptosis in virus-infected mammalian cells corresponds to its ability to inhibit apoptosis in *C. sonorensis* cells. This suggests that the anti-apoptotic CsIAP1 protein interacts with homologous components of the intrinsic apoptosis pathway present in mammalian cells and the core apoptosis pathway present in insects.

The BIR domains of IAP proteins bind directly to caspases to inhibit them and they are therefore essential for the anti-apoptotic property of IAP proteins. In contrast, several IAP proteins do not require their C-terminal RING motif to inhibit cell death and may therefore have different functions for different IAP proteins (Ditzel et al., 2008; Berthelet and Dubrez, 2013; Budhidarmo and Day, 2015). Mutagenesis showed that both the BIR2 and RING domains, but not the BIR1 domain, of CsIAP1 is required for anti-apoptotic activity. In this regard, it is interesting to note that studies on insect IAP proteins with multiple BIR domains have indicated that although the BIR domains are similar in domain architecture and sequence, they are functionally different. For example, in *D. melanogaster* DIAP1, binding of initiator and effector caspases is accomplished by the BIR2 and BIR1 domains, respectively (Chai et al., 2003; Tenev et al., 2005). However, in AeIAP1 of *Ae. aegypti*, the effector and initiator caspases bind to the BIR1 domain (Wang and Clem, 2011). Although further investigation is required, the results of the present study suggest that analogous to AeIAP1, the BIR2 domain of CsIAP1 is responsible for interaction with caspases while the RING domain may be required for promoting caspase ubiquination, which can result in caspase degradation via the proteasome (Wilson et al., 2002; Chai et al., 2003; Vaux and Silke, 2005). Notably, putative orthologues of the *D. melanogaster* initiator caspase Dronc and effector caspase Drice have been identified in the *C. sonorensis* transcriptome (Mills et al., 2015). Cloning and characterization of the putative caspases from *C. sonorensis* should shed new light on the specific target of CsIAP1 and would contribute to a more detailed understanding of the apoptosis pathway in *C. sonorensis*.

In contrast to mammalian cells, AHSV and BTV cause a non-lytic persistent infection in adult *Culicoides* midges and midge-derived cell lines (Mellor et al., 2000; Mortola et al., 2004; Stassen et al., 2012), even though *C. sonorensis* cells, as shown in this study, have a functional apoptosis pathway. This raises a number of questions; most importantly, why does

orbivirus infection not cause apoptosis in *C. sonorensis* midges and cells? Studies on mosquito vector competence for arboviruses have indicated that an antiviral apoptotic response can occur in mosquitoes that do not have the ability to vector a particular virus (Vaidyanathan and Scott, 2006; Girard et al., 2007; Kelly et al., 2012) and has led to the suggestion that apoptosis may be a key factor in determining vector competence (Clem, 2016). Conversely, it can therefore be surmised that there would be little or no apoptosis in successful virus-vector combinations. Indeed, cytopathological effects resulting from orbivirus infection in competent *Culicoides* vectors have not yet been reported in the literature (Mellor, 1990; Mellor et al., 2000). The lack of apoptosis in these specific orbivirus-*Culicoides* vector combinations may be a consequence of natural selection that favours the evolution of orbiviruses that are genetically more fit (i.e. do not induce apoptosis), since they stand an increased chance of being transmitted to the mammalian host (Mortola et al., 2004; O'Neill et al., 2015). Alternatively, it may also be that the level of orbivirus replication is modulated by other defences such as RNAi, which has recently been shown to target replication of BTV in *Culicoides* cells (Schnettler et al., 2013), thereby reducing virus replication to the point where it is not pro-apoptotic in permissive *Culicoides* vectors but still allows for productive infection and transmission.

In conclusion, the results indicate that CsIAP1 from *C. sonorensis* cells is functional as an anti-apoptotic protein that inhibits apoptosis in insect cells and protects mammalian cells from apoptosis induced by orbivirus infection. More work will be required to determine the exact mechanism and proteins involved in the apoptosis pathway in *C. sonorensis*, but this study allows further investigation into this process. Such knowledge will not only enhance our understanding of apoptosis regulation in this important disease vector, but also help to better understand the interactions between orbiviruses and *C. sonorensis* and allow for enhanced disease control methods based on the biology of this vector species.

Acknowledgments

This work was supported by the University of Pretoria's Institutional Research Theme Programme (Grant AOU999) and the National Research Foundation, South Africa (Grant 81068). Graduate bursary support was received from the National Research Foundation. We thank Miss A. Conradie for the pJET-S8 plasmid DNA and Mr. F. Wege for technical support with cell culture.

References

Berthelet, J., Dubrez, L., 2013. Regulation of apoptosis by inhibitors of apoptosis (IAPs). Cells 2, 163-187.

Budhidarmo, R., Day, C.L., 2015. IAPs: Modular regulators of cell signalling. Sem. Cell Dev. Biol. 39, 80-90.

Carpenter, S., Mellor, P.S., Torr, S.J., 2008. Control techniques for *Culicoides* biting midges and their application in the U.K. and northwestern Palaearctic. Med. Vet. Entomol. 22, 175-187.

Chai, J., Yan, N., Huh, J.R., Wu, J-W., Li, W., Hay, B.A., Shi, Y., 2003. Molecular mechanism of Reaper-Grim-Hid-mediated suppression of DIAP1-dependent Dronc ubiquitination. Nature Struct. Biol. 10, 892-898.

Chowdhury, I., Tharakan, B., Bhat, G.K., 2008. Caspases – An update. Comp. Biochem. Physiol. Part B, 151, 10-27.

Clem, R.J., 2016. Arboviruses and apoptosis: the role of cell death in determining vector competence. J. Gen. Virol. 97, 1033-1036.

Deveraux, Q.L., Takahashi, R., Salvesen, G.S., Reed, J.C., 1997. X-linked IAP is a direct inhibitor of cell-death proteases. Nature 388, 300-304.

Ditzel, M., Broemer, M., Tenev, T., Bolduc, C., Lee, T.V., Rigbolt, K.T., Elliott, R., Zvelebil, M., Blagoev, B., Bergmann, A., Meier, P., 2008. Inactivation of effector caspases through non-degradative polyubiquitylation. Mol. Cell 32, 540-553.

Girard, Y.A., Schneider, B.S., McGee, C.E., Wen, J., Han, V.C., Popov, V., Mason, P.W., Higgs, S., 2007. Salivary gland morphology and virus transmission during long-term cytopathologic West Nile virus infection in *Culex* mosquitoes. Am. J. Trop. Med. Hyg. 76, 118-128.

Hall, T.A., 1999. BioEdit: a user-friendly biological sequence alignment editor and analysis program for Windows 95/98NT. Nucleic Acids Symp. Ser. 41, 95-98.

Hay, B.A., Guo, M., 2006. Caspase-dependent cell death in *Drosophila*. Annu. Rev. Cell Dev. Biol. 22, 623-650.

Kean, J., Rainey, S.M., McFarlane, M., Donald, C.L., Schnettler, E., Kohl, A., Pondeville, E., 2015. Fighting arbovirus transmission: natural and engineered control of vector competence in *Aedes* mosquitoes. Insects 6, 236-278.

Kelly, E.M., Moon, D.C., Bowers, D.F., 2012. Apoptosis in mosquito salivary glands: Sindbis virus-associated and tissue homeostasis. J. Gen. Virol. 93, 2419-2424.

Li, J., Yuan, J., 2008. Caspases in apoptosis and beyond. Oncogene 27, 6194-6206.

Li, Q., Li., H., Blitvich, B.J., Zhang, J., 2007. The *Aedes albopictus* inhibitor of apoptosis 1 gene protects vertebrate cells from bluetongue virus-induced apoptosis. Insect Mol. Biol. 16, 93-105.

Liu, Q., Clem, R.J., 2011. Defining the core apoptosis pathway in the mosquito disease vector *Aedes aegypti*: the roles of *iap1*, *ark*, *dronc*, and effector caspases. Apoptosis 16, 105-113.

Mace, P.D., Shirley, S., Day, C.L., 2010. Assembling the building blocks: structure and function of inhibitor of apoptosis proteins. Cell Death Differ. 17, 46-53.

Manole, V., Laurinmäki, P., Van Wyngaardt, W., Potgieter, C.A., Wright, I.M., Venter, G.J., Van Dijk, A.A., Sewell, B.T., Butcher, S.J., 2012. Structural insight into African horse sickness virus infection. J. Virol. 86, 7858-7866.

Mellor, P.S., 1990. The replication of bluetongue virus in *Culicoides* vectors. Curr. Top. Microbiol. Immunol. 162, 143-161.

Mellor, P.S., Boorman, J., Baylis, M., 2000. *Culicoides* biting midges: their role as arbovirus vectors. Annu. Rev. Entomol. 45, 307-340.

Mellor, P.S., Mertens, P.P., 2009. Bluetongue. Biology of animal infections. Academic Press, Amsterdam, Netherlands.

Mills, M.K., Nayduch, D., Michel, K., 2015. Inducing RNA interference in the arbovirus vector, *Culicoides sonorensis*. Insect Mol. Biol. 24, 105-114.

Mortola, E., Noad, R., Roy, P., 2004. Bluetongue virus outer capsid proteins are sufficient to trigger apoptosis in mammalian cells. J. Virol. 78, 2875-2883.

Muro, I., Hay, B.A., Clem, R.J., 2002. The *Drosophila* DIAP1 protein is required to prevent accumulation of a continuously generated, processed form of the apical caspase DRONC. J. Biol. Chem. 277, 49644-49650.

Nagaleekar, V.K., Tiwari, A.K., Kataria, R.S., Bais, M.V., Ravindra, P.V., Kumar, S., 2007. Bluetongue virus induces apoptosis in cultures of mammalian cells by both caspase-dependent extrinsic and intrinsic pathways. Arch. Virol. 152, 1751-1756.

O'Neill, K., Olson, B.J., Huang, N., Unis, D., Clem, R.J. 2015. Rapid selection against arbovirus-induced apoptosis during infection of a mosquito vector. Proc. Natl. Acad. Sci. USA 112, 1152-1161.

Pretorius, J.M., Huismans, H., Theron, J., 2015. Establishment of an entirely plasmid-based reverse genetics system for bluetongue virus. Virology 486, 71-77.

Roy, N., Deveraux, Q.L., Takahashi, R., Salvesen, G.S., Reed, J.C., 1997. The c-IAP-1 and c-IAP-2 proteins are direct inhibitors of specific caspases. EMBO J. 16, 6914-6925.

Roy, P., 2008. Functional mapping of bluetongue virus proteins and their interactions with host proteins during virus replication. Cell Biochem. Biophys. 50, 143-157.

Salvesen, G.S., Duckett, C.S., 2002. IAP proteins: blocking the road to death's door. Nature Rev. Mol. Cell Biol. 3, 401-410.

Sambrook, J., Russell, D.W., 2001. Molecular cloning, a laboratory manual, 3rd ed. Cold Spring Harbour, Cold Spring Harbour Laboratory Press.

Schnettler, E., Ratinier, M., Watson, M., Shaw, A.E., McFarlane, M., Varela, M., Elliot, R.M., Palmarini, M., Kohla, A., 2013. RNA interference targets arbovirus replication in *Culicoides* cells. J. Virol. 87, 2441-2454.

Sim, S., Jupatanakul, N., Dimopoulos, G., 2014. Mosquito immunity against arboviruses. Viruses 6, 4479-4504.

Srinivasula, S.M., Ashwell, J.D., 2008. IAPs: what's in a name? Mol. Cell 30, 123-135.

Stassen, L., Huismans, H., Theron, J., 2012. African horse sickness virus induces apoptosis in cultured mammalian cells. Virus Res. 163, 385-389.

Stassen, L., Vermaak, E., Theron, J., 2014. African horse sickness, an equine disease of emerging global significance, in: Paz-Silva, A., Sol Arias Vázquez, M., Sánchez-Andrade Fernández R. (Eds.), Horses: Breeding, Health Disorders and Effects on Performance and Behaviour, Nova Publishers, New York, pp. 145-170.

Stewart, M.E., Roy, P., 2010. Role of cellular caspases, nuclear factor-kappa B and interferon regulatory factors in Bluetongue virus infection and cell fate. Virol. J. 7, 1-16.

Tenev, T., Zachariou, A., Wilson, R., Ditzel, M., Meier, P., 2005. IAPs are functionally non-equivalent and regulate effector caspases through distinct mechanisms. Nature Cell Biol. 7, 70-77.

Timmer, J.C., Salvesen, G.S., 2007. Caspase substrates. Cell Death Differ. 14, 66-72.

Vaidyanathan, R., Scott, T.W., 2006. Apoptosis in mosquito midgut epithelia associated with West Nile virus infection. Apoptosis 11, 1643-1651.

Vaux, D.L., Silke, J., 2005. IAPs, RINGs and ubiquitylation. Nature Rev. Mol. Cell Biol. 6, 287-297.

Vermaak, E., Theron, J., 2015. Virus uncoating is required for apoptosis induction in cultured mammalian cells infected with African horse sickness virus. J. Gen. Virol. 96, 1811-1820.

Vermaak, E., Conradie, A.M., Maree, F.F., Theron, J., 2016. African horse sickness virus infects BSR cells through macropinocytosis. Virology 497, 217-232.

Wang, H., Clem, R.J., 2011. The role of IAP antagonist proteins in the core apoptosis pathway of the mosquito disease vector *Aedes aegypti*. Apoptosis 16, 235-248.

Wechsler, S.J., McHolland, L.E., Tabachnick, W.J., 1989. Cell lines from *Culicoides variipennis* (Diptera: Ceratopogonidae) support replication of bluetongue virus. J. Inv. Pathol. 54, 385-393.

Wilson, A., Mellor, P.S., Szmaragd, C., Mertens, P.P.C., 2009. Adaptive strategies of African horse sickness virus to facilitate vector transmission. Vet. Res. 40, 16.

Wilson, A.J., Mellor, P.S., 2009. Bluetongue in Europe: Past, present and future. Phil. Trans. R. Soc. B. 364, 2669-2681.

Wilson, R., Goyal, L., Ditzel, M., Zachariou, A., Baker, D.A., Agapite, J., Steller, H., Meier, P., 2002. The DIAP1 RING finger mediates ubiquitination of Dronc and is indispensable for regulating apoptosis. Nature Cell Biol. 4, 445-450.

Wyllie, A.H., 1997. Apoptosis: an overview. Brit. Med. Bull. 53, 451-465.

Zhang, H., Li, H.C., Miao, X.X., 2013. Feasibility, limitation and possible solutions of RNAi-based technology for insect pest control. Insect Sci. 20, 15-30.

Figure legends

Fig. 1. Silencing of Cs*iap*1 induces apoptosis in KC cells. (A) Total RNA was extracted from Cs*iap*1 dsRNA-treated, control (AHSV-4 S8) dsRNA-treated and untreated (Unt) KC cells at the indicated times post-treatment and semi-quantitative RT-PCR was performed using Cs*iap*1 gene-specific and Hsp60-specific primers. (B) Micrographs of Cs*iap*1 dsRNA-treated KC cells depicting morphological characteristics typical of apoptosis at the indicated times post-treatment. Control (AHSV-4 S8) dsRNA-treated and untreated KC cells are shown for comparative purposes. Cells were photographed at 40× magnification and representative results are shown. (C) DNA fragmentation analysis of Cs*iap*1 dsRNA-treated, control (AHSV-4 S8) dsRNA-treated and untreated KC cells at 24 and 48 h post-treatment. (D) Cytoplasmic extracts from control dsRNA- and Cs*iap*1 dsRNA-treated, as well as untreated KC cells, at 24 and 48 h post-treatment, were used to determine caspase-3-like activity using an ELISA assay. The data are means ± SD of three independent experiments and are presented as the fold increase in caspase-3-like activity (* $P \leq 0.05$, by a Student's *t* test).

Fig. 2. Rescue of apoptosis induced in BSR mammalian cells by infection with AHSV-4 or BTV-10. (A) Micrographs of BSR and BSR-Cs*iap*1 cells infected with AHSV-4 or BTV-10 showing morphological characteristics of apoptosis at 24 and 48 h post-infection. Mock-infected BSR and BSR-Cs*iap*1 cells are shown for comparative purposes. Cells were photographed at 20× magnification and representative results are shown. (B) Enrichment of nucleosomes in the cytoplasm of BSR and BSR-Cs*iap*1 cells infected with AHSV-4 or BTV-10. Cytoplasmic extracts were prepared at the indicated time points from mock-infected and virus-infected cells, and the release of free nucleosomes into the cytoplasm was determined by an ELISA assay. The data were used to calculate the nucleosome enrichment factor in virus-infected cells and are presented as the means ± SD of three independent experiments (* $P \leq 0.05$, by a Student's *t* test). (C) Caspase-3 activity in BSR and BSR-Cs*iap*1 cells infected with AHSV-4 or BTV-10. Cytoplasmic extracts were prepared from mock-infected and virus-infected cells at 24 and 48 h post-infection, and the caspase-3 activity determined using an ELISA assay. Data are shown as means ± SD of three independent experiments and are presented as the fold increase in capase-3 activity in the virus-infected cells (* $P \leq 0.05$, by a Student's *t* test).

Fig. 3. Virus growth curves. BSR and BSR-Cs*iap*1 cells were infected with AHSV-4 or BTV-10 at a MOI of 0.1 pfu/cell. The titre of the respective viruses at different times post-infection, as indicated in the figure, was determined by plaque assays in BSR cells. The data are means ± SD of three independent experiments, each performed in duplicate.

Fig. 4. CsIAP1 suppresses caspase-9, but not caspase-8. The activity of (A) caspase-8 and (B) caspase-9 was determined using caspase-specific ELISA assays by making use of cytoplasmic extracts prepared from mock-infected and virus-infected BSR and BSR-Cs*iap*1 cells at the indicated time points. The data are means ± SD of three independent experiments and are presented as the fold increase in the activity of the respective caspases in the virus-infected cells (* $P \leq 0.05$, by a Student's *t* test).

Fig. 5. The CsIAP1 BIR2 and RING domains are required to suppress apoptosis mediated by caspase-9. (A) Micrographs of BSR-Cs*iap*1, BSR-Cs*iap*1ΔBIR1, BSR-Cs*iap*1ΔBIR2 and BSR-Cs*iap*1ΔRING cells infected with AHSV-4 showing morphological characteristics of apoptosis at 48 h post-infection. Mock-infected and virus-infected BSR cells are shown for comparative purposes. Cells were photographed at 20× magnification and representative results are shown. The activity of (B) caspase-3 and (C) caspase-9 in the respective infected cell lines was determined at 48 h post-infection using caspase-specific ELISA assays by making use of cytoplasmic extracts prepared from mock-infected and virus- infected cells at the indicated time points. The data are means ± SD of three independent experiments and are presented as the fold increase in the activity of the respective caspases in the virus-infected cells (* $P \leq 0.05$, by a Student's *t* test).

Figure 1

A

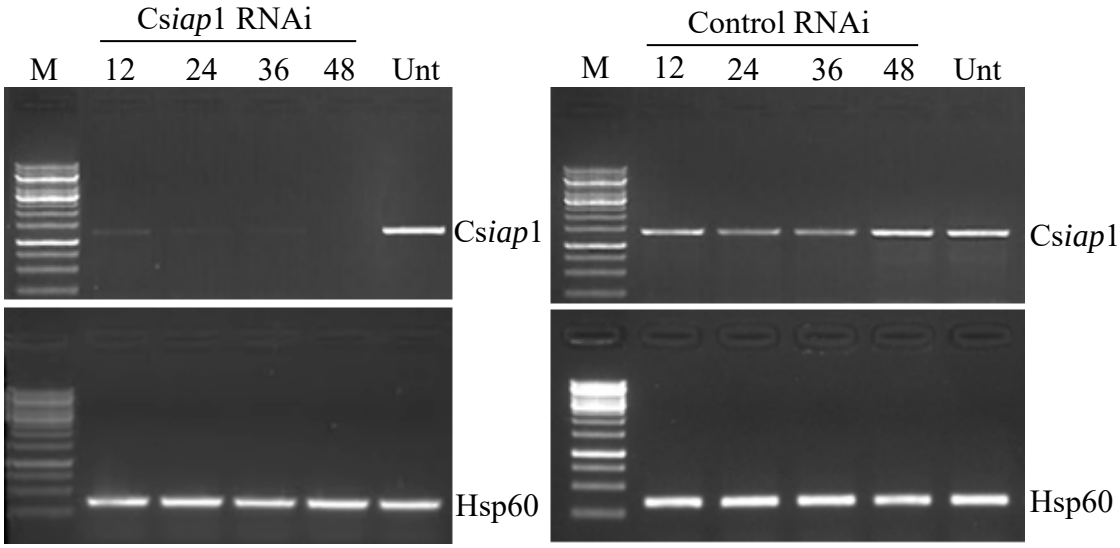
Csiap1 RNAi
M
12
24
36
48
Unt
Csiap1
Hsp60
Control RNAi
M
12
24
36
48
Unt
Csiap1
Hsp60

B

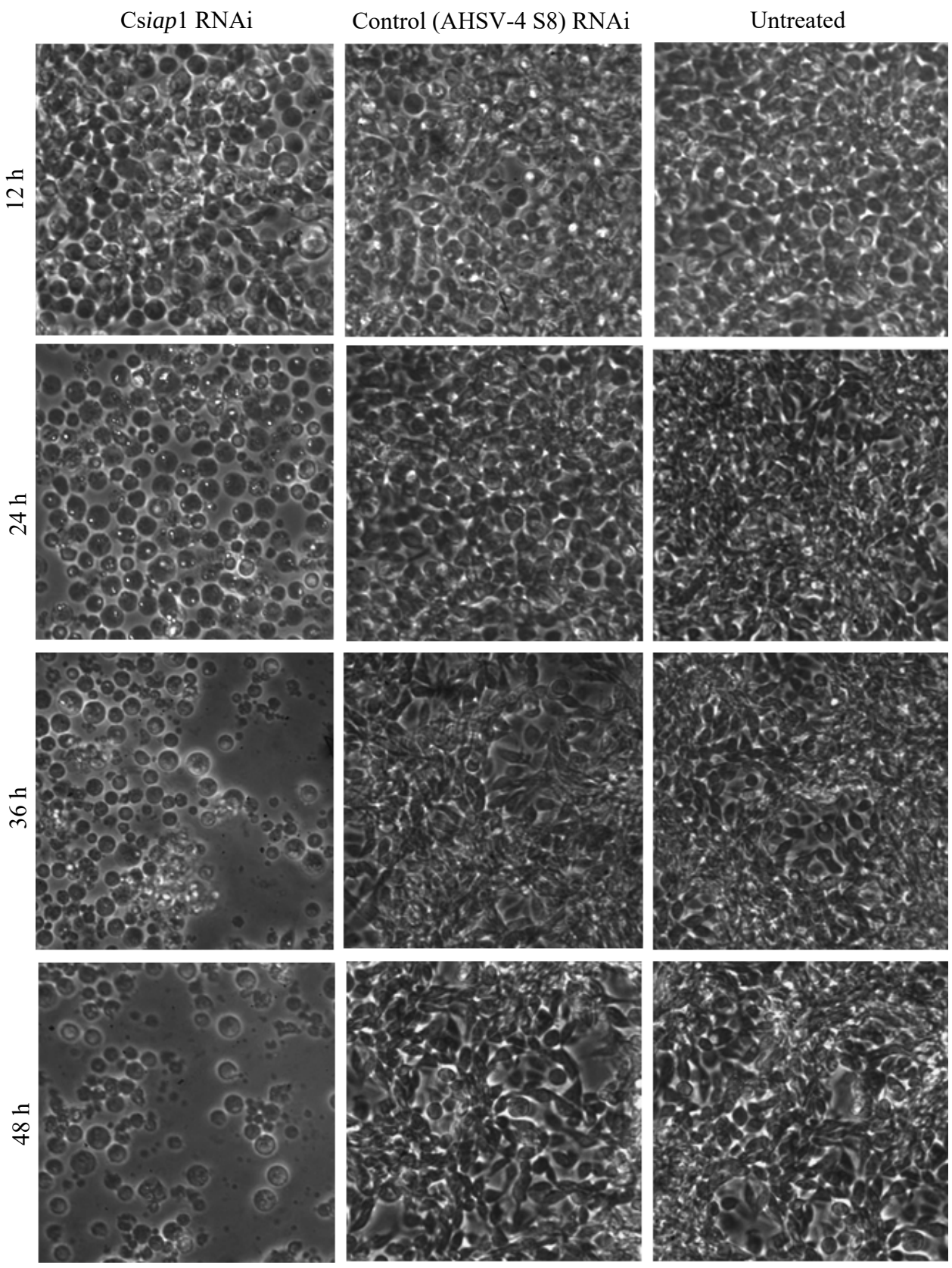

C

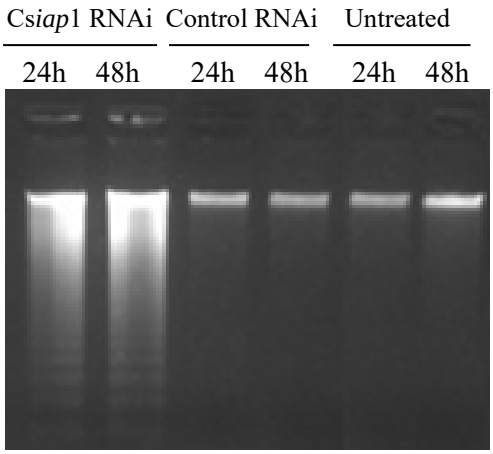
Csiap1 RNAi
Control RNAi
Untreated
24h
48h
24h
48h
24h
48h

D

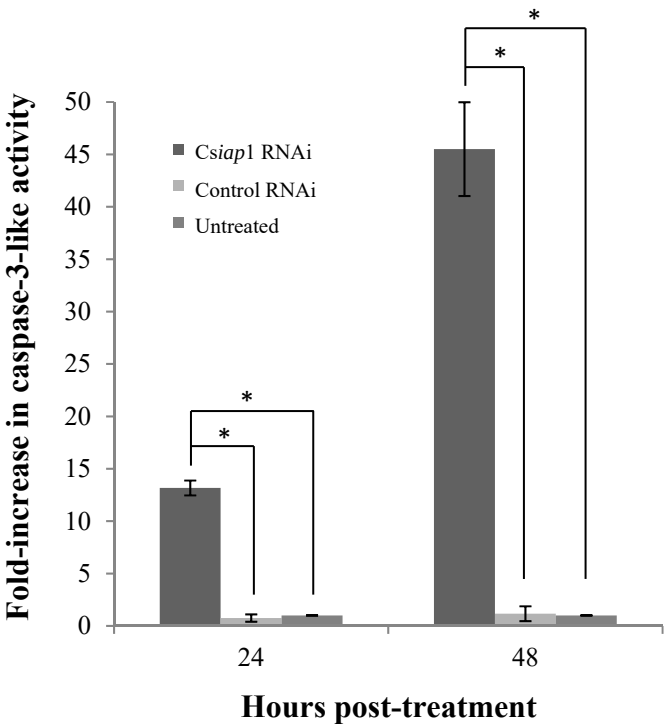
Fold-increase in caspase-3-like activity
50
45
40
35
30
25
20
15
10
5
0
Csiap1 RNAi
Control RNAi
Untreated
*
*
*
*
24
48
Hours post-treatment

Figure 2

A

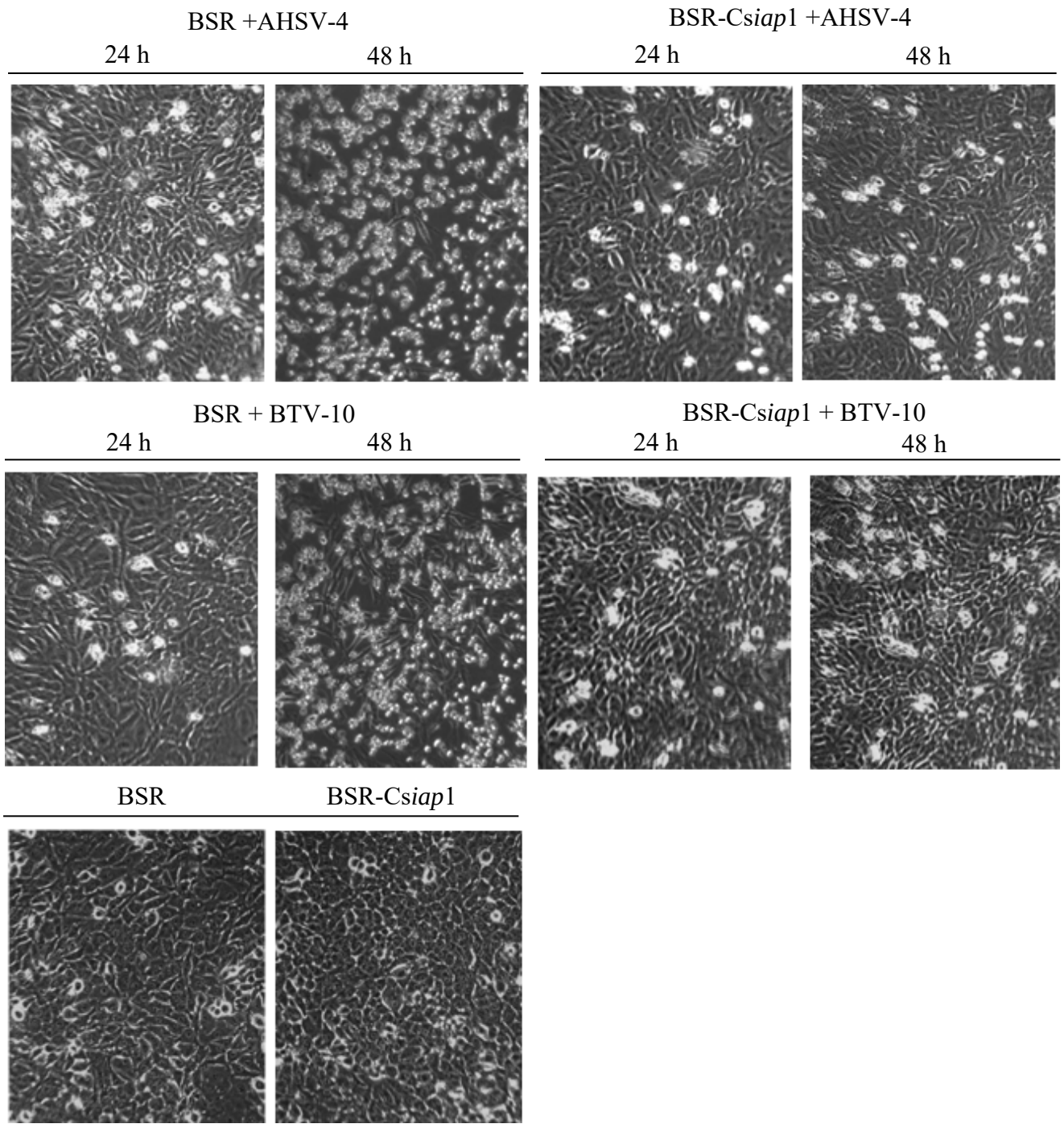
BSR +AHSV-4
24 h
48 h
BSR-Csiap1 +AHSV-4
24 h
48 h
BSR + BTV-10
24 h
48 h
BSR-Csiap1 + BTV-10
24 h
48 h
BSR
BSR-Csiap1

B

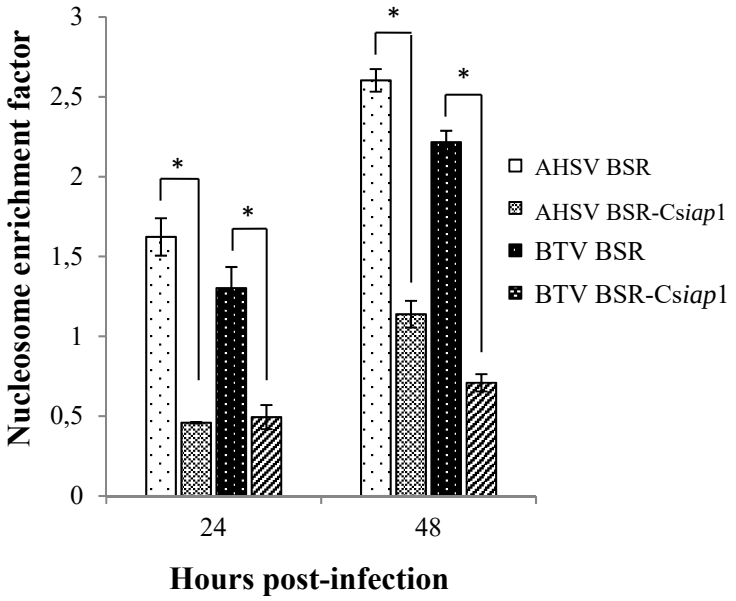
Nucleosome enrichment factor
3
2,5
2
1,5
1
0,5
0
*
*
*
*
24
48
Hours post-infection
AHSV BSR
AHSV BSR-Csiap1
BTV BSR
BTV BSR-Csiap1

C

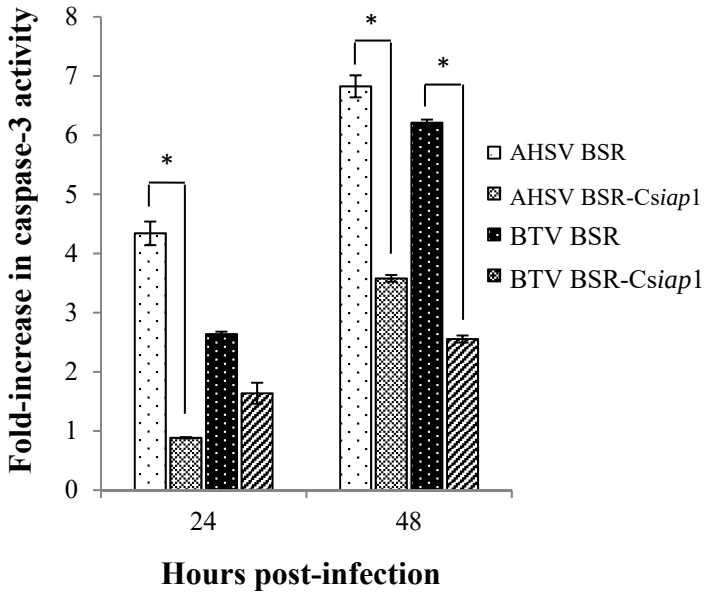
Fold-increase in caspase-3 activity
8
7
6
5
4
3
2
1
0
*
*
*
*
24
48
Hours post-infection
AHSV BSR
AHSV BSR-Csiap1
BTV BSR
BTV BSR-Csiap1

Figure 3

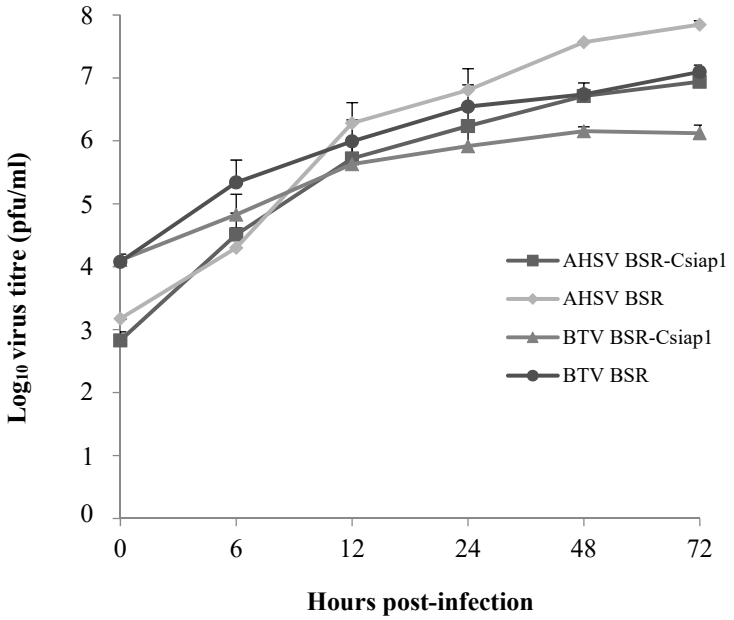
8
7
6
5
4
3
2
1
0
Log10 virus titre (pfu/ml)
0
6
12
24
48
72
Hours post-infection
AHSV BSR-Csiap1
AHSV BSR
BTV BSR-Csiap1
BTV BSR

Figure 4

A

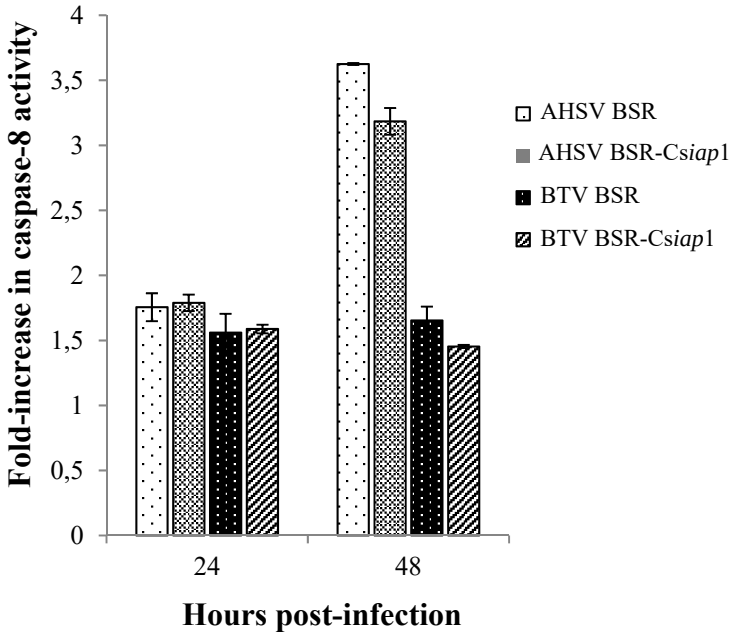
Fold-increase in caspase-8 activity
4
3,5
3
2,5
2
1,5
1
0,5
0
24
48
Hours post-infection
AHSV BSR
AHSV BSR-Csiap1
BTV BSR
BTV BSR-Csiap1

B

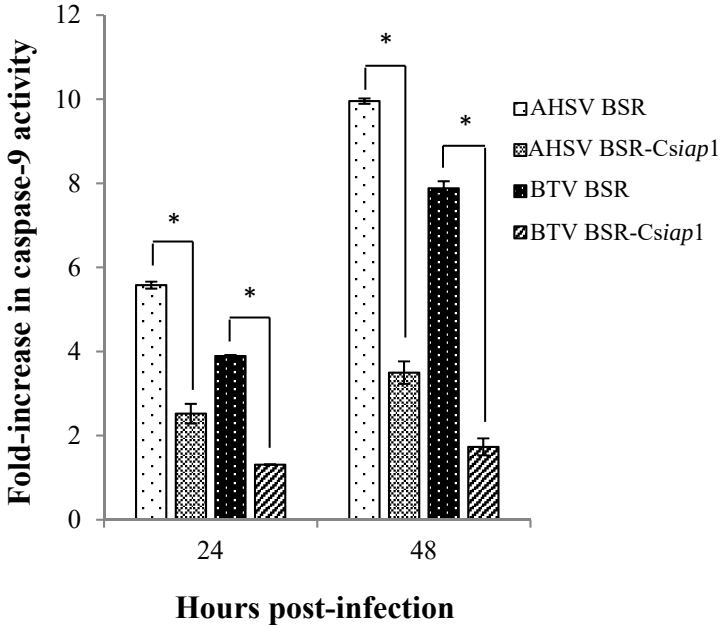
Fold-increase in caspase-9 activity
12
10
8
6
4
2
0
*
*
*
*
24
48
Hours post-infection
AHSV BSR
AHSV BSR-Csiap1
BTV BSR
BTV BSR-Csiap1

Figure 5

A

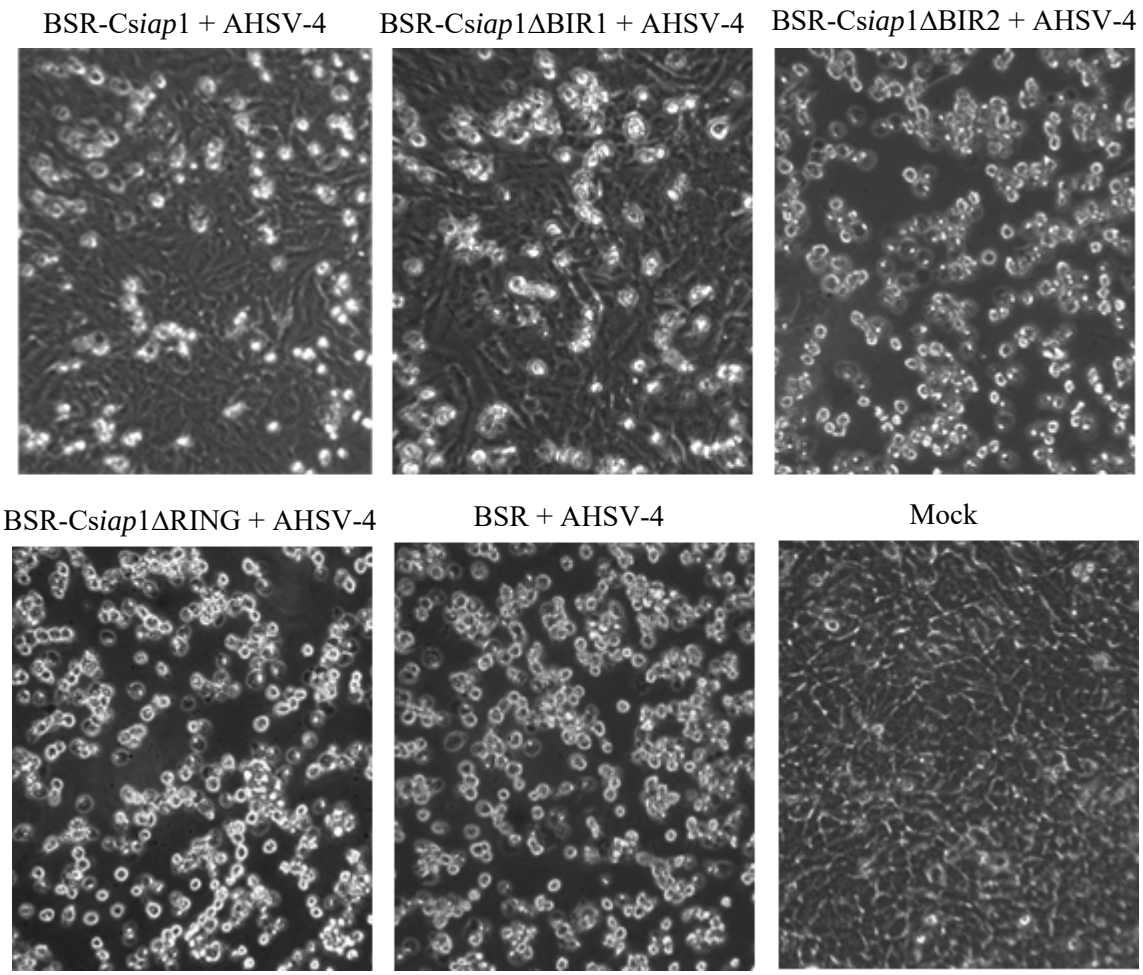
BSR-Csiap1 + AHSV-4
BSR-Csiap1ΔBIR1 + AHSV-4
BSR-Csiap1ΔBIR2 + AHSV-4
BSR-Csiap1ΔRING + AHSV-4
BSR + AHSV-4
Mock

B

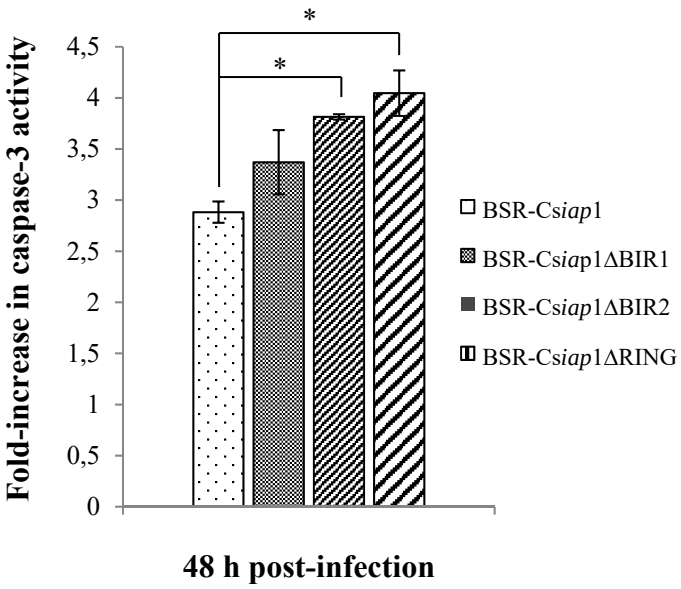
Fold-increase in caspase-3 activity
4,5
4
3,5
3
2,5
2
1,5
1
0,5
0
*
*
BSR-Csiap1
BSR-Csiap1ΔBIR1
BSR-Csiap1ΔBIR2
BSR-Csiap1ΔRING
48 h post-infection

C

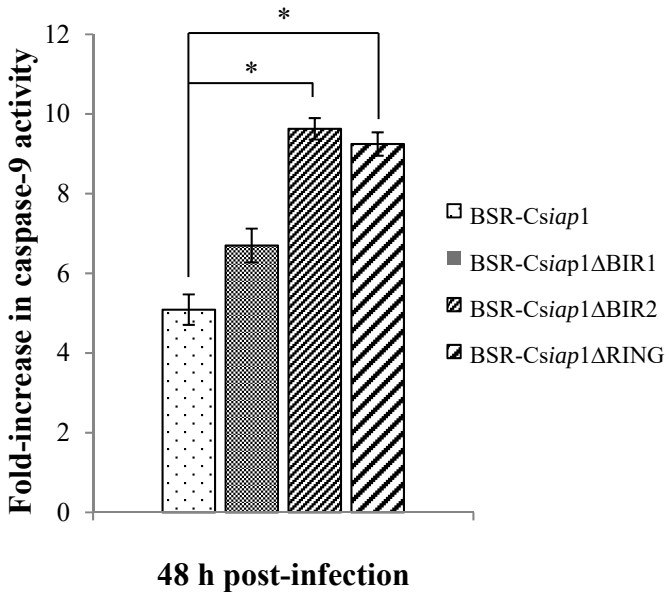
Fold-increase in caspase-9 activity
12
10
8
6
4
2
0
*
*
BSR-Csiap1
BSR-Csiap1ΔBIR1
BSR-Csiap1ΔBIR2
BSR-Csiap1ΔRING
48 h post-infection

Supplementary Figure 1

A

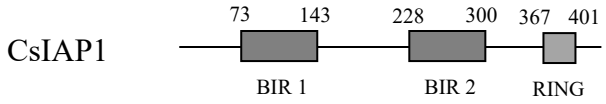

B

MAPCYKVLKTKMATLTRIIKDTFQKHNDEIDNKDNKEKEKDPYDFMNPRNSTQTSPSPPASP
RNVPTTITGL**NKEKQRRLTFSNWNCPTTDKFLLAQIGFYFIGPTDLVKCYFCNVEIGMW**
QPEDNPVEEHLRWSPNCPLLHGRETSNEPIDAEALKRILPTISYDTCGIRAGNSIPPGSYPEISI
NHPNESNIRDLSPQPSSSSGSSQQIDITPTSMMAHRNEHPE**FAIESHRLVSYEDWPKTMKQK**
PKELAEAGFCNTGKGDRVACFSCGGGLKDWEEMDVPWEQHAMWYSKCEYLKLMKG
QEFIDEILARKSSPPSSYTEASNLGTSVAGSSKDEVKKPNEVAKCAGVAMEEPKTAAVSDSK
M**CKICYECEYNTAFFPCGHIIACAKCASSVTKCPYC**RQPFTKVMRVYFS

C

```
                10        20        30        40        50        60        70
        ....|....|....|....|....|....|....|....|....|....|....|....|....|.
CsIAP1  NKEKQRRLTFSNWNCPTTDKFLLAQIGFYFIGPTDLVKCYFCNVEIGMWQPEDNPVEEHLRWSPNCPLLHG
DIAP1   NREETRLKTFTDWPLDWLDKRQLAQTGMYFTHAGDKVKCFFCGVEIGCWEQEDQPVPEHQRWSPNCPLLRR
AtIAP1  HTEVARLDSFRNWTVLFITKAELARYGFYYVGPNDMVKCYFCRVEIGLWEPNDNVLSEHLRWSPYCPLLRK
AaIAP1  HTEVSRLESFRDWMVPFISKTELARYGFYYVGPNDMVKCYFCRVEIGLWEQNDNVLSEHLRWSPYCPLLRK
AeIAP1  HTEVARLESFRGWMVSFISKTELARYGFYYVGPNDMVKCYFCRVEIGLWEPNDNVLSEHLRWSPYCPLLRK
         . *   * :*  *      *  **: *:*:    * ***:** **** *: :*: : ** **** ****:
```

D

```
               10        20        30        40        50        60        70
       ....|....|....|....|....|....|....|....|....|....|....|....|....|...
CsIAP1 FAIESHRLVSYEDWPKTMKQKPKELAEAGFCNTGKGDRVACFSCGGGLKDWEEMDVPWEQHAMWYSKCEYLKL
DIAP1  YAIETARLRTFEAWPRNLKQKPHQLAEAGFFYTGVGDRVRCFSCGGGLMDWNDNDEPWEQHALWLSQCRFVKL
AtIAP1 YAIEAKRLESYEDWPKFMKQKPKELSDAGFFYTGKGDRVKCFSCGGGLKDWEAEDEPWEQHAMWYSNCEYLKL
AaIAP1 YAIEAKRLECYEDWPKFMKQKPKELSDAGFFYPGKSDRVKCFSCGGGLKDWEAEDEPWEQHAMWYSNCEYLKL
AeIAP1 YAIEAKRLESYEDWPKFMKQKPKELSDAGFFYTGKSDRVKCFSCGGGLKDWEAEDEPWEQHAMWYSNCEYLKL
       :***: **  :* **: :****::*::***   * .*** ******** **:  * ******:* *:*.::**
```

E

```
                10        20        30
        ....|....|....|....|....|....|....|
CsIAP1  CKICYECEYNTAFFPCGHIIACAKCASSVTKCPYC
DIAP1   CKICYGAEYNTAFLPCGHVVACAKCASSVTKCPLC
AtIAP1  CKICYVNEYNTAFSPCGHVVACAKCASSVTKCPLC
AaIAP1  CKICYVNEYNTAFSPCGHVVACAKCASSVTKCPLC
AeIAP1  CKICYVNEYNTAFSPCGHVVACAKCASSVTKCPLC
        *****  ****** ****::************ *
```

Supplementary Fig. S1. Predicted domain topology and amino acid sequence of CsIAP1. (A) The BIR and RING domains of CsIAP1 are depicted. (B) The predicted amino acid sequence of CsIAP1 is presented. Bold text indicates the BIR1, BIR2 and RING domains. Sequence alignments of the BIR1 (C), BIR2 (D) and RING (E) domains of CsIAP1 with the corresponding domains of other insect IAP family members are shown. The signature sequences $CX_2CX_{16}HX_{6-8}C$ in the BIRs and C_3HC_4 in the RING domain are underlined. The GenBank accession numbers of sequences used for the alignments are: *C. sonorensis* IAP1 (CsIAP1) KT246121, *D. melanogaster* IAP1 (DIAP1) L49440.1, *Ae. triseriatus* IAP1 (AtIAP1) AF447592.1, *Ae. albopictus* IAP1 (AaIAP1) AF488809.1, and *Ae. aegypti* IAP1 (AeIAP1) DQ993355.1.

Supplementary Figure 2

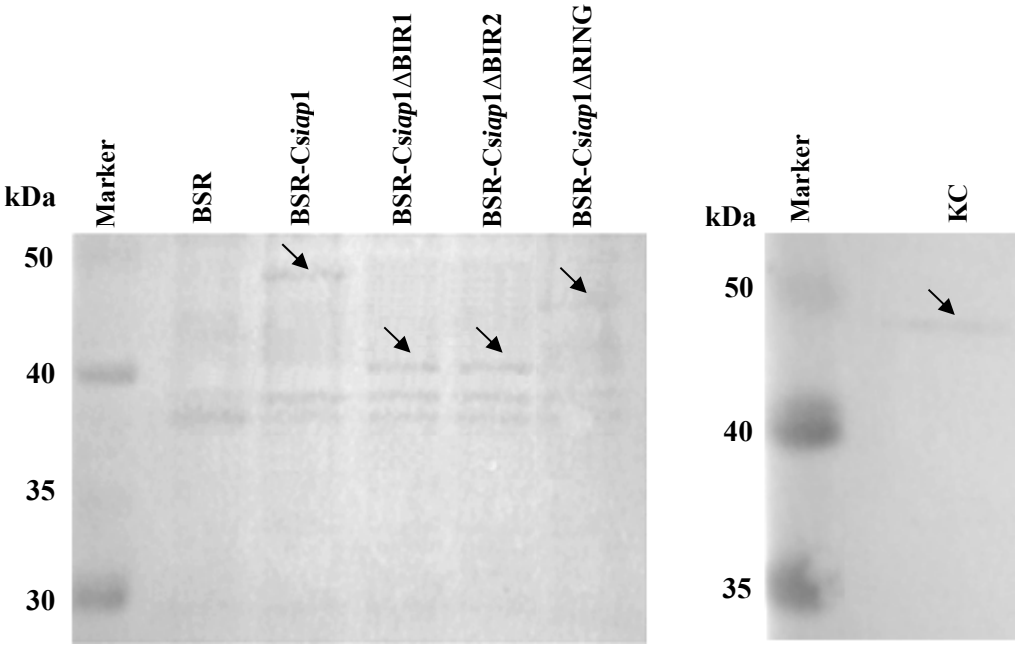

Supplementary Fig. S2. Expression of CsIAP1 and CsIAP1 deletion mutants in stable BSR cell lines. Immunoblot analysis with an anti-CsIAP antibody was performed to confirm expression of the full-length CsIAP1 protein and of ΔBIR1, ΔBIR2 and ΔRING deletion mutants of CsIAP in stable BSR cell lines. Arrows denote the position of the respective proteins. *C. sonorensis* (KC) cells were included positive control. The sizes of the Spectra Multicolor Broad Range Protein Ladder (Thermo Fisher) are indicated to the left of the figure (M).